Modeling of the $P700^+$ Charge Recombination Kinetics with Phylloquinone and Plastoquinone-9 in the A_1 Site of Photosystem I

Vladimir P. Shinkarev,* Boris Zybailov,† Ilya R. Vassiliev,† and John H. Golbeck†
*Department of Biochemistry, University of Illinois, Urbana, Illinois 61801, and †Department of Biochemistry and Molecular Biology, The Pennsylvania State University, University Park, Pennsylvania 16802 USA

ABSTRACT Light activation of photosystem I (PS I) induces electron transfer from the excited primary electron donor P700 (a special pair of chlorophyll *a*/*a′* molecules) to three iron–sulfur clusters, F_X, F_A, and F_B via acceptors A_0 (a monomeric chlorophyll *a*) and A_1 (phylloquinone). PS I complexes isolated from *menA* and *menB* mutants contain plastoquinone-9 rather than phylloquinone in the A_1 site and show altered rates of forward electron transfer from A_1^- to $[F_A/F_B]$ and altered rates of back electron transfer from $[F_A/F_B]^-$ to $P700^+$ (Semenov, A. Y., et al., *J. Biol. Chem.* 275:23429–23438, 2000). To identify the modified electron transfer steps, we studied the kinetics of flash-induced $P700^+$ reduction in PS I that contains either an intact set or a subset of iron–sulfur clusters F_X, F_A, and F_B and with the A_1 binding site occupied by phylloquinone or plastoquinone-9. A modeling of the forward and backward electron transfer kinetics in P700–F_A/F_B complexes, P700–F_X cores, and P700–A_1 cores shows that the replacement of phylloquinone by plastoquinone-9 induces a decrease in the free energy gap between A_1 and F_A/F_B from ~ -205 mV in wild-type PS I to ~ -70 mV in *menA* PS I. The +135 mV increase in the midpoint potential of A_1 explains the acceleration in the rate of $P700^+$ dark reduction in *menA* PS I, and the resulting uphill electron transfer from A_1 to F_X in *menA* PS I explains the absence of a contribution from F_X^- to the reduction of $P700^+$. This fully quantitative description of PS I relates electron transfer rates, equilibrium constants, and redox potentials, and can be used to predict changes in these parameters upon substitution of electron transfer cofactors.

INTRODUCTION

Photosystem I (PS I) of oxygenic photosynthesis is a membrane-bound pigment–protein complex that functions as a light-dependent plastocyanin (or cytochrome c_6): ferredoxin (or flavodoxin) oxidoreductase. Light-induced electron transfer takes place in a series of reactions between neighboring cofactors that are embedded in this complex. The primary electron carriers include a symmetrical set of six chlorophyll molecules, two phylloquinones and three iron–sulfur clusters. Of these, the primary electron donor is P700, a special pair of chlorophyll *a*/*a′* molecules, and the primary electron acceptor is A_0, a monomeric chlorophyll *a*. A phylloquinone molecule (A_1), and three [4Fe–4S] clusters (F_X, F_A, and F_B) operate as intermediate and terminal electron acceptors, respectively. The cofactors P700, A_0, A_1, and F_X are bound to the two main polypeptides, PsaA and PsaB, whereas the terminal electron acceptors F_A and F_B are bound to the small PsaC subunit (reviewed in Brettel, 1997; Fromme, 1999; Golbeck, 1999; Manna and Chitnis, 1999; Ke, 2001; Brettel and Leibl, 2001; and Vassiliev et al., 2001a).

The x-ray structure analysis of PS I crystals at 4-Å resolution (Klukas et al., 1999a, 1999b), and more recently at 2.5-Å resolution (Jordan et al., 2001), has revealed the position of the cofactors, including the two phylloquinone molecules and the three iron–sulfur clusters F_X, F_B, and F_A (Fig. 1). The reaction center chlorophylls and the quinones in PS I have a two-fold symmetrical arrangement similar to that of purple bacteria, in which a dimer of bacteriochlorophyll molecules transfers the electron via two "monomeric" chlorin cofactors to the quinone.

The phylloquinone acceptor can be extracted using organic solvents, and its function can be reconstituted using artificial quinones and a variety of quinoid compounds (Itoh et al., 1987; Iwaki and Itoh, 1991a, 1991b; Iwaki and Itoh, 1994; Iwaki et al., 1996). In situ values of the quinones correlate with their $E_{1/2}$ values determined polarographically in dimethylformamide (DMF): E_m(in situ) = $E_{1/2}$(in DMF) − 310 mV (Iwaki et al., 1996). The estimated energy of reorganization for electron transfer from A_0 to A_1 is ~0.3 eV (Iwaki et al. 1996), in sharp contrast with the estimated energy of reorganization for electron transfer from $A_1 \rightarrow F_X$ of 0.8 to 1 eV (Schlodder et al., 1998).

Submitted April 7, 2002 and accepted for publication July 17, 2002.

Address reprint requests to John H. Golbeck, Dept. of Biochemistry and Molecular Biology, The Pennsylvania State University, S.310 Frear Hall, University Park, PA 16802. Tel.: 814-865-1162; Fax: 814-863-7024; E-mail: jhg5@psu.edu; or Vladimir P. Shinkarev, Dept. of Biochemistry, Univ. of Illinois at Urbana–Champaign, 156 Davenport Hall, 607 Mathews Ave., Urbana, IL 61801-3838. Tel.: 217-333 8725; Fax: 217-244 6615; E-mail: vshinkar@uiuc.edu.

Dr. Vassiliev's present address is Signature BioScience, Inc., 475 Brannan St., San Francisco, CA 94107.

Abbreviations used: F_A, Cubane iron–sulfur center bound by cysteines 21, 48, 51, and 54 on the PsaC subunit; F_B, cubane iron–sulfur center bound by cysteines 11, 14, 17, and 58 on the PsaC subunit; F_X, cubane iron–sulfur center bound to PsaA and to PsaB subunits; L_{XA}, the equilibrium constant of electron transfer between F_X and F_A; P700, primary donor of electrons in Photosystem I; wild-type PS I, PS I complex containing phylloquinone, F_X, F_A, and F_B clusters, isolated using *n*-dodecyl-β-D-maltoside; mutant PS I, PS I complex containing plastoquinone-9, F_X, F_A, and F_B clusters, isolated using *n*-dodecyl-β-D-maltoside; ΔA_{832}, photoinduced absorbance change at 832 nm.

0006-3495/02/12/2885/13 $2.00

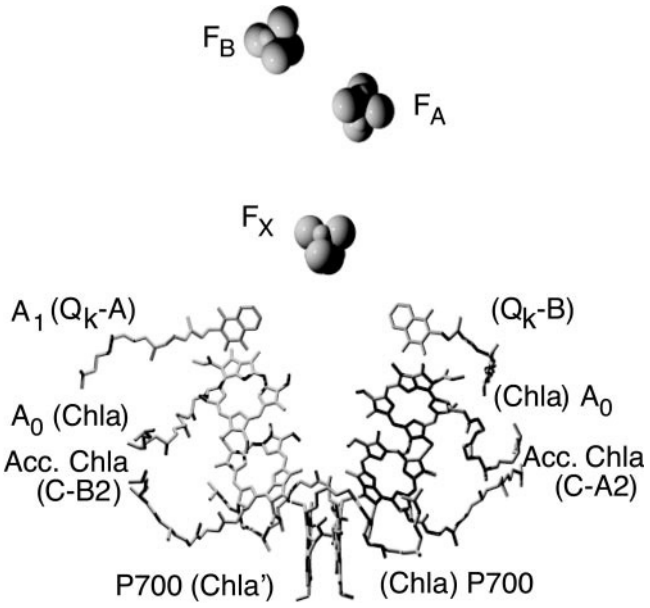

FIGURE 1 Structural model of PS I. The primary electron donor, P700, is comprised of Chl *a* molecule eC-B1 and Chl *a′* molecule eC-A1. The Chl *a* molecule spectroscopically identified as the primary acceptor A_0 is probably eC-A3, and the phylloquinone molecule spectroscopically identified as the secondary acceptor A_1 is probably Q_K-A. The [4Fe-4S] cluster Fx is bound by two cysteines from PsaA and two cysteines from PsaB. The F_A and F_B [4Fe-4S] clusters are bound to the PsaC subunit.

A number of new constructs allows genetic modification of the cofactors on the acceptor side of PS I and provides new and unique tools for the analysis of the kinetics of electron transport in PS I complexes. Johnson et al. (2000) constructed *menA* and *menB* interruption mutants in *Synechocystis* sp. PCC 6803, in which plastoquinone-9 is present in the A_1 site of PS I (Zybailov et al., 2000; Semenov et al., 2000). The mutants retain a photochemically active PS I complex and can grow photosynthetically even in the absence of phylloquinone. Phylloquinone can be restored into the A_1 site by adding authentic phylloquinone or its precursors, 2-carboxy-1,4-naphthoquinone or 2-methyl-1,4-naphthoquinone, to growing *menB* (but not *menA*) mutant cells (Johnson et al., 2001).

Shen et al. (2002b) constructed a *rubA* interruption mutant in *Synechococcus* sp. PCC 7002, which lacks the iron–sulfur clusters F_X, F_A, and F_B (Shen et al., 2002a). Recently a *menB/rubA* double mutant was constructed in *Synechococcus* sp. PCC 7002 (B. Zybailov, Y. Sakuragi, G. Shen, D. Bryant, and J. Golbeck, manuscript in preparation) which lacks the iron–sulfur clusters F_X, F_B, and F_A and has plastoquinone-9 in the A_1 binding site. These new biological methods constitute a useful adjunct to chemical methods to remove the iron–sulfur clusters and to incorporate novel quinones into the A_1 site of PS I.

Here, we analyze the kinetics of $P700^+$ dark reduction in PS I complexes that contain either an intact set or a subset of the iron–sulfur clusters F_X, F_B, and F_A, with A_1 site occupied by phylloquinone or plastoquinone-9. Our analysis shows that, in wild-type PS I complexes that contain phylloquinone in the A_1 site, the free energy gap between A_1 and iron–sulfur clusters F_A/F_B is ~ -205 mV. In mutant PS I complexes that contain plastoquinone-9 in the A_1 site, the free energy gap between A_1 and iron–sulfur clusters F_A/F_B is ~ -70 mV. The acceleration in the rate of $P700^+$ dark reduction in plastoquinone-containing PS I and the absence of a contribution from F_X to the reduction of $P700^+$ in the absence of iron–sulfur clusters F_A and F_B can be explained by the +135-mV change in the midpoint potential of A_1.

MATERIALS AND METHODS

Construction and growth of mutant cells

The *menA* mutant was constructed in *Synechocystis* sp. PCC 6803 as described in Johnson et al. (2001) and grown phototoautotrophically under low levels of illumination. The phenotype of this mutant is that PS I contains plastoquinone-9 in the A_1 site. The *rubA* mutant was constructed in *Synechococcus* sp. PCC 7002 (Shen et al., 2002b) and grown photoheterotrophically using glycerol as a carbon source. The phenotype of this mutant is that PS I lacks the iron–sulfur clusters F_X, F_B, and F_A (Shen et al., 2002a). The *menB/rubA* double mutant was constructed in *Synechococcus* sp. PCC 7002 (B. Zybailov, Y. Sakuragi, G. Shen, D. Bryant, and J. Golbeck, manuscript in preparation) and grown photoheterotrophically using glycerol as a carbon source. The phenotype of this mutant is that PS I contains plastoquinone-9 in the A_1 site, and additionally lacks the iron–sulfur clusters F_X, F_B, and F_A.

Isolation of PS I complexes

PS I complexes from the wild-type, and the *menA* and *menB/rubA* mutants were isolated from membranes using *n*-dodecyl-β-D-maltoside and purified by sucrose gradient ultracentrifugation as described in Golbeck (1995). The PS I complexes were resuspended in Tris buffer (0.05 M Tris, pH 8.3) with 15% glycerol, frozen as small aliquots in liquid nitrogen, and stored at −95°C. PS I complexes were stripped of the F_A and F_B iron–sulfur clusters by removal of the PsaC protein using 6.8 M urea as described in Golbeck (1995). The presence of the F_X cluster was verified in the PsaC-stripped preparations by slow freezing to 77 K in the light to photoaccumulate P700 F_X^- followed by EPR spectroscopy at 8 K.

Time-resolved absorbance spectroscopy

Samples for optical experiments were in quartz cuvettes with air-tight stoppers. The reaction medium contained 25 mM Tris buffer (pH 8.3), 4 μM 2,6-dichlorophenol-indophenol (DCPIP), 10 mM sodium ascorbate, and 0.04% *n*-dodecyl-β-D-maltoside. The chlorophyll concentration was 50 μg/ml. Methyl viologen was added where indicated. The solutions were prepared in an anaerobic chamber using oxygen-free distilled water, air being substituted in a Thunberg tube by high-purity nitrogen. All chemicals were obtained from Sigma (St. Louis, MO).

The kinetics of absorbance changes at 832 nm (ΔA_{832}) were measured in 10 × 4 mm cuvette using a spectrophotometer described in Vassiliev et al. (2001a). In experiments with wild-type samples, the measuring beam (power, 30 mW; λ, 832 nm) was provided by a PMT-25 laser diode assembly (Power Technology Inc., Little Rock, AR). In experiments with mutant samples that require faster time resolution, the measuring beam was

provided by a titanium-sapphire laser (model TI-SPB, Schwartz Electro-Optics, Orlando, FL) tuned to 832 nm (power, ~200 mW) pumped with a diode-pumped, frequency-doubled CW Nd:YVO4 laser (Millenia, Spectra Physics, Mountain View, CA) at 5.4-W output power. Single turnover flashes were provided by a frequency-doubled (λ, 532 nm), Q-switched (FWHM, 10 ns) Nd-YAG laser model DCR-11 (Spectra Physics). A flash energy of 3.6 mJ was sufficient for saturation of P700 photochemistry without producing significant antenna chlorophyll triplets. The intervals between the actinic flashes were 50 s.

Data analysis using a stretched exponential

The ΔA_{832} kinetics shown in Figs. 2 and 3 reflect the dark reduction of $P700^+$, and are presented on a logarithmic time scale so that the charge recombination from different electron acceptors can be easily visualized. The distribution of time constants can be described as $f(\tau) = \int_0^\infty F(\tau, 0)\exp(-t/\tau)\,dt$, where $F(\tau, 0)$ is the distribution function of amplitudes over the continuum of time constants. An alternative method of fitting the kinetics with fewer numbers of components is provided by the Kohlrausch law (Kohlrausch, 1854, 1863), or stretched-multiexponential, in which each component is represented as $A(t) = A_0\exp((-t/\tau)^\beta)$ and in which the stretch parameter β varies between 0 and 1 (for discussion, see Vassiliev et al., 2001a, 2001b). This equation represents a robust solution of a general equation for kinetics with a distributed time constant. In the case when $\beta = 1$, the equation turns into a simple exponential. It is particularly useful for PS I kinetics, in which nonexponential kinetics may reflect different conformational states of the reaction center (Vassiliev et al., 1997). The stretched exponential is used in this study to simplify the analysis of the kinetic components that are ascribed to a particular electron acceptor.

RESULTS

Measurement of the kinetics of $P700^+$ dark reduction

The relationship of a lifetime of $P700^+$ dark reduction and a particular electron acceptor can be established using preparations lacking some or all of the iron–sulfur clusters, F_X, F_B, and F_A. Ideally, the monomolecular back reaction between a particular reduced acceptor and $P700^+$ should follow monoexponential kinetics, but, in many instances, the experimental data are best fitted by two or more closely-spaced kinetic components (Vassiliev et al., 1997) that are folded here into a single stretched exponential without losing the quality of the fit (see Figs. 2 and 3). The value of the stretch factor β varies between 0 and 1 (with 1 being a simple exponential), and it provides a measure of the heterogeneity of the kinetics. The nature of this heterogeneity in the dark reduction of $P700^+$ is not fully understood, but it may be related to existence of different conformational (sub)states in the PS I complex (Vassiliev et al., 1997). Such a heterogeneity has been reported in PS I (Schlodder et al., 1998) and in reaction clusters from purple bacteria (McMahon et al., 1998). Additional phases in purified PS I complexes can also arise from differential damage to the iron–sulfur clusters during isolation, but these are usually identifiable by their distinctive lifetimes. The decay of the triplet state of chlorophyll (Brettel and Golbeck, 1995; Vassiliev et al., 1997) can further contribute to a microsecond kinetic phase, but this assignment can be readily verified by studying the flash-saturation profile and wavelength dependence in the near-IR. The proposed participation of two different branches of cofactors in electron transport in PS I has been recently suggested as an additional source of heterogeneity of the measured kinetics (Guergova-Kuras et al., 2001). Even though several decay rates may exist for a particular forward or backward reaction, we will use only one rate constant to simplify the analysis in this paper. Usually this chosen rate constant is the weighted average of the two rate constants. A more comprehensive analysis, which takes into account multiple rate constants and the possibility of multiple pathways, will be forthcoming in a separate work.

Kinetics of $P700^+$ dark reduction in PS I complexes with phylloquinone in the A_1 site

Figure 2 *A* shows typical kinetics of flash-induced absorbance changes at 832 nm in wild-type (phylloquinone-containing) PS I complexes from *Synechocystis* sp. PCC 6803 in the presence of DCPIP and ascorbate. The stretched multiexponential fit of the kinetics shows three different components with characteristic lifetimes of 2.2 ms (0.94), 107 ms (0.93), and 2.0 s (0.76) with relative amplitudes of ~5%, 68%, and 28%, respectively (the stretch factor is in parenthesis). The minor, 2.2-ms kinetic phase may be due to a subset of PS I complexes in which PsaC has been lost during isolation (see Fig. 2 *B*). The 2.0-s kinetic phase is due to forward electron donation by DCPIP in PS I complexes in which the electron has been lost from the iron–sulfur clusters, presumably by donation to dioxygen (Vassiliev et al., 1997).

Figure 2 *B* shows the kinetics of flash-induced absorbance changes in a wild-type PS I core stripped of PsaC, and hence devoid of the F_A and F_B iron–sulfur clusters. The stretched multiexponential fit of the kinetics shows four different components with characteristics lifetimes of 11.6 μs (0.73), 192 μs (0.73), 971 μs (0.85), and 426 ms (0.49), and amplitudes ~20%, 20%, 48%, and 5%, respectively. The kinetic phase with an ~1.0-ms lifetime has been shown by optical and EPR spectroscopy to represent the backreaction of $P700^+$ with F_X^- (Golbeck, 1995), and agrees with the lifetime of $P700^+$ measured in a *psaC* interruption mutant in *Synechocystis* sp. PCC 6803 (Yu et al., 1995). The kinetic phases of ~12 and 200 μs in a 1:1 ratio represents the backreaction of $P700^+$ with A_1^- (Vassiliev et al., 1997; also, see Fig. 1 *C*) in PS I complexes in which F_X has inadvertently been destroyed. The kinetic phase with a 426-ms lifetime probably represents a population of PS I complexes in which PsaC has not been removed.

Figure 2 *C* shows the kinetics of flash-induced absorbance changes in a PS I core isolated from the *rubA* mutant that contains phylloquinone in the A_1 site, but no F_X, F_A, or

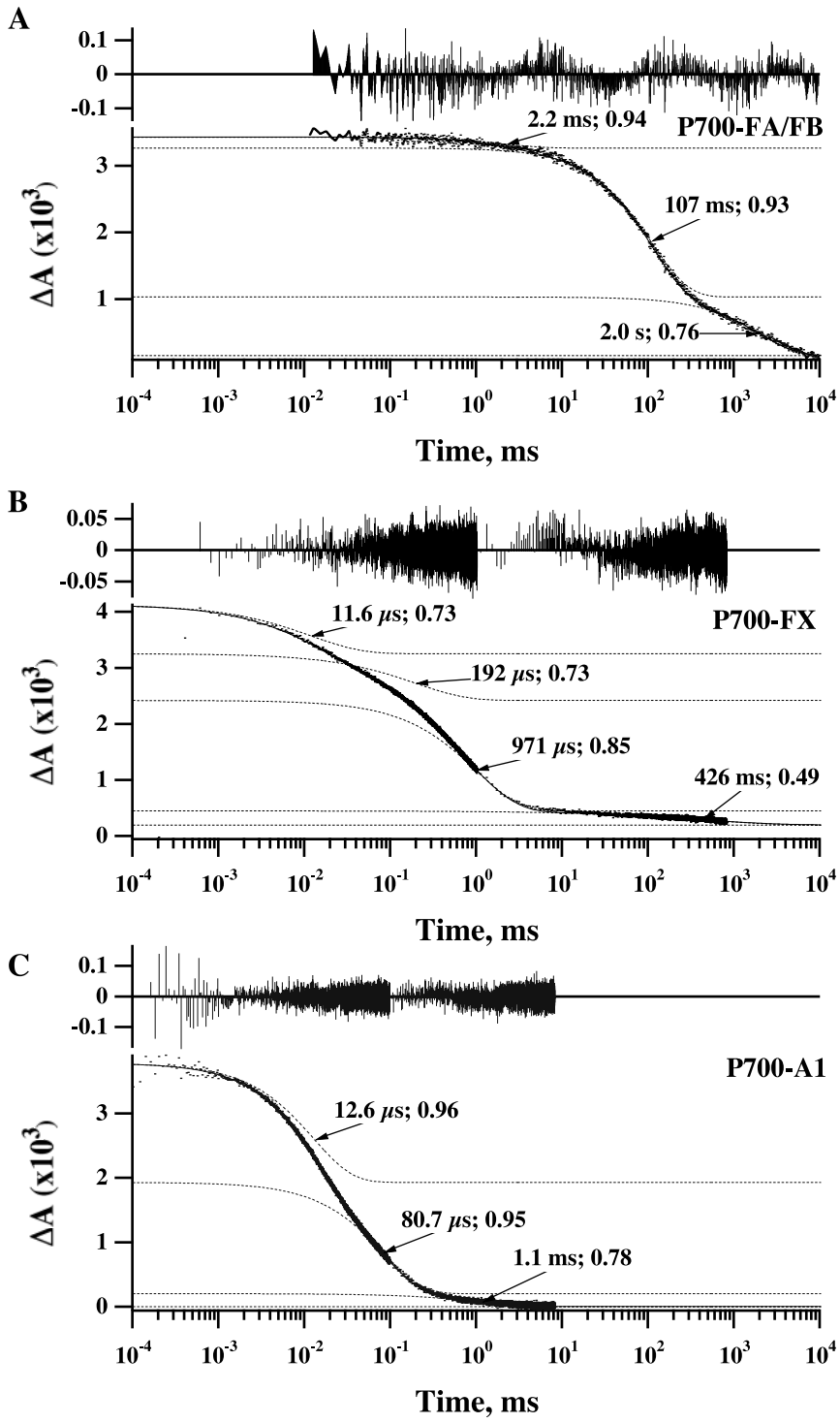

FIGURE 2 Kinetics of absorbance changes at 832 nm in wild-type PS I complexes with phylloquinone in the A_1 site. (*A*) Intact PS I complex with F_X, F_B, and F_A present (wild-type). (*B*) PS I core lacking F_A and F_B, (prepared by chemically removing PsaC from the wild-type with urea). (*C*) PS I core lacking F_X, F_A, and F_B (prepared from the *rubA* mutant). Reaction medium: (*top*) 25 mM Tris buffer (pH 8.3), 0.04% *n*-dodecyl-β-D-maltoside, 4 μM DCPIP, and 10 mM sodium ascorbate. Each individual component of the stretched multiexponential fit is plotted with a vertical offset relative to the next component (with a longer lifetime) or the baseline, the offset being equal to the amplitude of the latter component. The values indicate the (1/*e*) lifetime and the stretch parameter.

F_B iron–sulfur clusters. The stretched multiexponential fit of the kinetics shows three different components with characteristic lifetimes of 12.6 μs (0.96), 80.7 μs (0.95), and 1.1 ms (0.78) with relative amplitudes of 49.7%, 43.1%, and 4.1%, respectively. The two microsecond components have been shown by optical and EPR spectroscopy to represent the backreaction of $P700^+$ with A_1^- (Shen et al., 2000a). These lifetimes are similar to the ~10- and 110-μs lifetimes measured in a chemically prepared P700-A_1 core that also lacks F_X, F_A, and F_B. Both kinetic phases show spectral signatures in the near-UV characteristic of the semiquinone anion radical (Brettel and Golbeck, 1995).

Kinetics of $P700^+$ dark reduction in PS I complexes with plastoquinone in the A_1 site

Figure 3 *A* shows typical kinetics of flash-induced absorbance changes at 832 nm in *menA* (plastoquinone-containing) PS I complexes from *Synechocystis* sp. PCC 6803 in the presence of DCPIP and ascorbate. The stretched multiexponential fit of the kinetics shows two different components with characteristic lifetimes of 4.1 μs (1.00) and 2.9 ms (1.00) with relative amplitudes of 9% and 80%, respectively. Optical and EPR studies (Semenov et al., 2000) have shown that the ~3-ms component represents the backreaction of $P700^+$ with a reduced iron–sulfur cluster, most probably $[F_A/F_B]^-$.

Figure 3 *B* shows the kinetics of flash-induced absorbance changes in a *menA* PS I core stripped of PsaC, and hence devoid of the F_A and F_B iron–sulfur clusters. The stretched multiexponential fit of these kinetics shows four different components with characteristic lifetimes of 3 μs (0.81), 26 μs (0.59), 584 μs (0.82), and 1.7 ms (0.28), and amplitudes of 13%, 21%, 66%, and 20%, respectively. Optical studies in the near-UV at 315 nm show kinetics components with lifetimes of ~25 and 700 μs ascribed to a semiquinone anion radical (J. Golbeck, A. Semenov, and B. Diner, unpublished results). Thus, the 26- and 584-μs kinetic components in the stripped *menA* PS I core are assigned to the $P700^+$ A_1^- backreaction.

Figure 3 *C* shows the kinetics of flash-induced absorbance changes in a PS I core isolated from the *rubA/menB* double mutant that contains plastoquinone in the A_1 site, but no F_X, F_A, or F_B iron–sulfur clusters. The stretched multiexponential fit of the kinetics shows four different components with characteristic lifetimes of 2.5 μs (0.60), 26 μs (0.75), 362 μs (0.96), and 5.9 ms (0.93), with relative amplitudes of 17%, 14%, 54%, and 7%, respectively. The spectra of the 26- and 362-μs components have derivative-like absorbance changes between 400 and 600 nm ascribed to electrochromic bandshifts of pigments in the vicinity of A_1^-, i.e., β-carotene and chlorophyll (B. Zybailov, Y. Sakuragi, G. Shen, D. Bryant, and J. Golbeck, manuscript in preparation). Optical studies in the near-UV show kinetic components with lifetimes of ~15 and 400 μs with a spectrum between 250 and 340 nm, characteristic of a semiquinone anion radical (J. Golbeck, B. Zybailov, and B. Diner, unpublished results). Thus, the 26- and 362-μs kinetic components in the *rubA/menB* double mutant are assigned to the $P700^+$ A_1^- backreaction.

The similarity of the lifetimes and spectral characteristics of the 584- and 362-μs components in *menA* PS I cores with PsaC and F_X removed, compared to the lifetimes and spectral characteristics of the ≈1-ms and 10–100-μs components in similar wild-type PS I cores indicates significant changes in the energetics of the acceptor side of the *menA* PS I complexes. This phenomenon, and the acceleration in the backreaction in fully-intact *menA* PS I, can be explained by shift of the midpoint potential of A_1 in such a way that equilibrium between A_1 and F_X is shifted in favor of A_1 (see Discussion).

DISCUSSION

General expression for the rate constant of the flash-induced dark reduction of $P700^+$

To understand the kinetics of $P700^+$ dark reduction in wild-type and *menA* PS I complexes, we need to consider baseline information concerning the kinetics of electron transfer. Figure 4 shows the generally accepted scheme of flash-induced electron transfer in PS I. The rate constants and respective midpoint potentials are taken from the current literature and provide general guidance rather than exact values. They can be adjusted to fit the kinetics in a particular sample or strain, if needed. What is important here is that forward electron transfer at each successive step is faster than the back reaction to $P700^+$. Hence, we can assume the (quasi)equilibrium between different states of the PS I complex during dark reduction. The assumption of the (quasi)equilibrium between different states of the PS I complex is frequently used for the analysis of the electron transfer in PS I (see e.g., Iwaki and Itoh, 1994; Brettel, 1997). Using such assumption, the observed rate constant of P^+ dark reduction can be described by the general expression (Shinkarev and Wraight 1993),

$$k_P \approx k_{PP}[P^*] + k_{A_0P}[A_0^-] + k_{A_1P}[A_1^-] + k_{F_XP}[F_X^-] + k_{F_AP}[F_A^-] + k_{F_BP}[F_B^-]. \quad (1)$$

Here k_{pp} is the rate constant for P* deexcitation; k_{A_0P} is the rate constant of *direct* electron transfer from A_0^- to $P700^+$; k_{A_1P} is the rate constant of direct electron transfer from A_1^- to $P700^+$; k_{F_XP} is the rate constant of direct electron transfer from F_X^- to $P700^+$; k_{F_AP} is the rate constant of direct electron transfer from F_A^- to $P700^+$; and k_{F_BP} is the rate constant of direct electron transfer from F_B^- to $P700^+$.

Square brackets in Eq. 1 indicate the *relative* (per PS I complex) concentrations of the different states of PS I. Assuming (quasi)equilibrium between different states dur-

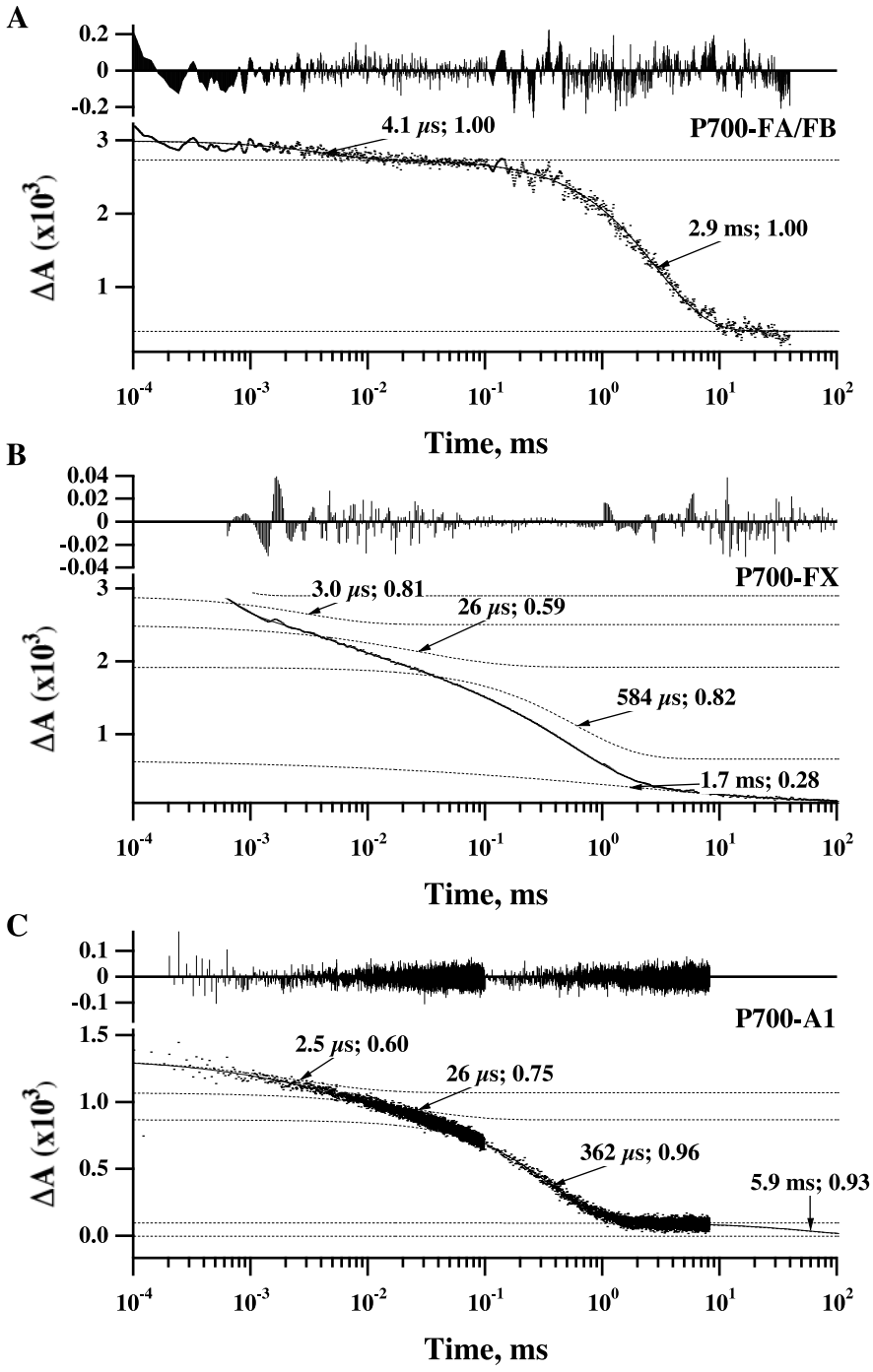

FIGURE 3 Kinetics of absorbance changes at 832 nm in *menA* PS I complexes with plastoquinone in the A_1 site. (*A*) Intact PS I complex with F_X, F_B, and F_A present (*menB* mutant). (*B*) PS I core lacking F_A and F_B (prepared by chemically removing PsaC from the *menB* mutant with urea). (*C*) PS I core lacking F_X, F_A, and F_B (prepared from the *rubA/menB* double mutant). Note that the relatively low ΔA is due to the inadvertent loss of a population of plastoquinone-9 from the A_1 binding site during detergent isolation (B. Zyabilov, Y. Sakuragi, G. Shen, D. Bryant, and J. Golbeck, manuscript in preparation). Reaction medium: 25 mM Tris buffer (pH 8.3), 0.04% *n*-dodecyl-β-D-maltoside, 4 μM DCPIP, and 10 mM sodium ascorbate. Each individual component of the stretched multiexponential fit is plotted with a vertical offset relative to the next component (with a longer lifetime) or the baseline, the offset being equal to the amplitude of the latter component. The values indicate the ($1/e$) lifetime and the stretch parameter.

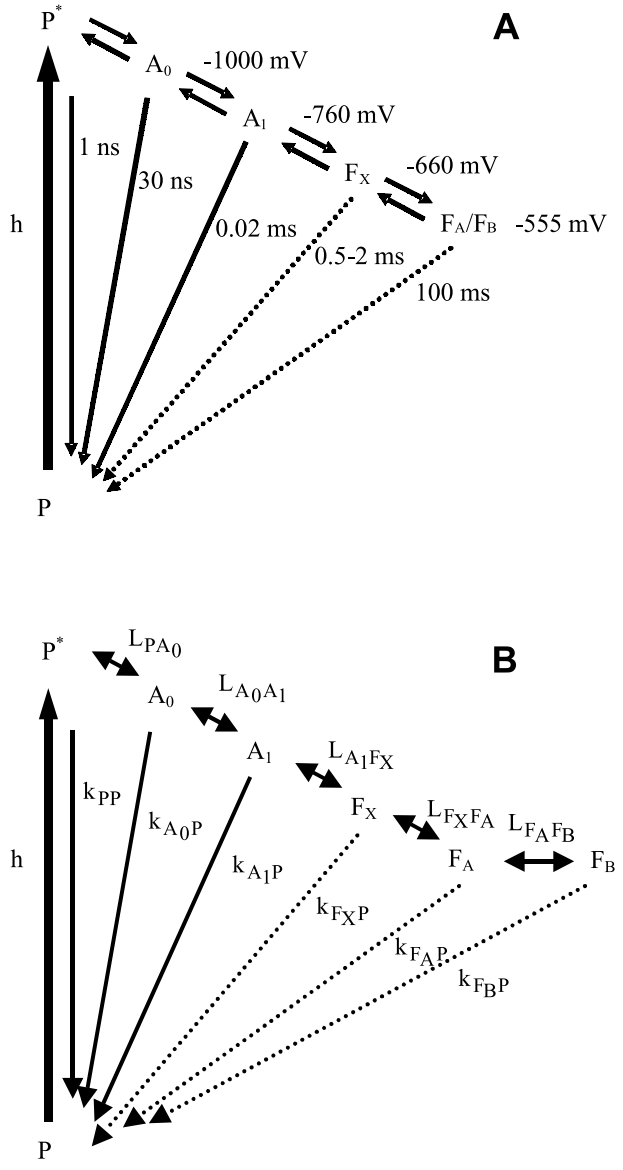

FIGURE 4. (*A*) Scheme of electron transport in PS I (reviewed in Brettel, (1997) and Ke, (2001)). Note that we depict the rate constant of direct electron transfer for reactions $A_0 \rightarrow P$, $A_1 \rightarrow P$. The indicated time for the reaction $F_A/F_B \rightarrow P$ corresponds to the indirect electron transfer via F_X. (*B*) Notations used for the rate and equilibrium constants. The values depicted for the redox potentials and backreaction times are taken from the literature, and are either experimentally determined or deduced from thermodynamic or kinetic arguments (i.e., the E_m of A_0 and A_1).

ing dark reduction, the relative concentrations of the components can be found as functions of an equilibrium constant of electron transfer between the components,

$$[P^*] \approx 1/Z, \quad [A_0^-] \approx L_{PA_0}/Z,$$

$$[A_1^-] \approx L_{PA_1}/Z, \quad [F_X^-] \approx L_{PF_X}/Z,$$

$$Z \approx 1 + L_{PA_0} + L_{PA_1} + L_{PF_X} + L_{PF_A} + L_{PF_B}. \qquad (2)$$

Here, L_{PA_0} is the equilibrium constant for electron transfer from P* to A_0, $L_{A_0}A_1$ is the equilibrium constant for electron transfer from A_0 to A_1, etc.

$$L_{PA_1} \approx L_{PA_0}L_{A_0A_1},$$

$$L_{PF_X} \approx L_{PA_0}L_{A_0A_1}L_{A_1F_X},$$

$$L_{PF_A} \approx L_{PA_0}L_{A_0A_1}L_{A_1F_X}L_{F_XF_A},$$

$$L_{PF_B} \approx L_{PA_0}L_{A_0A_1}L_{A_1F_X}L_{F_XF_A}L_{F_AF_B}$$

(see Fig. 4 *B* for a notation of the equilibrium constants between electron carriers).

The distance between F_A (F_B) and P700 provided by the x-ray crystal structure is so large (>30 Å (Jordan et al., 2001) that, based on the dependence of the logarithm of the rate constant on distance (Moser et al., 1995), we can ignore direct electron transfer between them and $P700^+$ on a millisecond time scale. Thus, electron transfer from F_A^- and F_B^- to $P700^+$ occurs indirectly via thermal repopulation of F_X, F_A, etc. Similarly, the edge-to-edge distance of 26–27 Å between F_X and P700 also indicates that the time of electron transfer from F_X^- to $P700^+$ should be seconds.

Assuming $k_{FAP} = 0$, $k_{FBP} = 0$, and $k_{FXP} = 0$, Eq. 1 for the observed rate constant of $P700^+$ dark decay can be rewritten in the simplified form,

$$k_P \approx k_{PP}[P^*] + k_{A_0P}[A_0^-] + k_{A_1P}[A_1^-]. \qquad (3)$$

Inserting the values of the relative concentrations of the different states from Eq. 2 into Eq. 3 gives the expression for the apparent rate constant of $P700^+$ dark reduction after a flash,

$$k_P = \frac{k_{PP} + k_{A_0P}L_{PA_0} + k_{A_1P}L_{PA_1}}{1 + L_{PA_0} + L_{PA_1} + L_{PF_X} + L_{PF_A} + L_{PF_B}}. \qquad (4)$$

This equation can be rewritten via the relevant free energy differences, $\Delta G_{XY} = -RT \ln(L_{XY})$,

$$k_P \approx (k_{PP} + k_{A_0P} \exp(-\Delta G_{PA_0}/RT) + k_{A_1P} \exp(-\Delta G_{PA_1}/RT)/Z. \qquad (5)$$

Both Eqs. 4 and 5 can be used as the starting point for the analysis of the changes of $P700^+$ dark reduction introduced by plastoquinone-9. We assume on the first iteration of this model that the absence of PsaC does not influence the thermodynamic or kinetic properties of F_X, and that the absence of F_X does not influence the thermodynamic kinetic properties of A_1.

Phylloquinone-containing PS I complexes

Flash-induced reactions of wild-type PS I in the absence of the F_A/F_B iron–sulfur clusters

In wild-type PS I without PsaC, F_X serves as the terminal electron acceptor. Flash-induced reactions are therefore

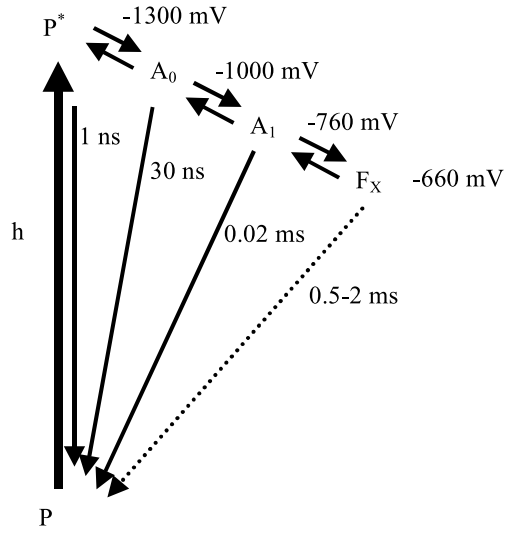

FIGURE 5 Scheme of electron transport in wild-type PS I in the absence of PsaC.

mainly limited to low-potential electron carriers on the acceptor side (Fig. 5) up to and including F_X.

The free energy difference for each transition is negative (each equilibrium constant in Eq. 4 is larger than 1). Because the energy gap between P* and F_X is largest (see Figure 5), the term $\exp(-\Delta G_{PF_X}/RT)$ plays a dominant role in the denominator of Eq. 5. So, by multiplying both numerator and denominator by $\exp(\Delta G_{PF_X}/RT)$ we have

$$(k_P^{Phy})_{no\ F_AF_B} \approx k_{PP}\exp(\Delta G_{PF_X}/RT) + k_{A_0P}\exp(\Delta G_{A_0F_X}/RT) + k_{A_1P}\exp(\Delta G_{A_1F_X}/RT). \quad (6)$$

This equation indicates the various routes of electron transfer that contribute to the effective rate constant of $P700^+$ decay. These routes include the thermal repopulation of A_1 (from F_X), followed by direct electron transfer from A_1 to $P700^+$ (the term $k_{A_1P}\exp(\Delta G_{A_1F_X}/RT)$); thermal repopulation of A_0 (from F_X), followed by direct electron transfer from A_0 to $P700^+$ (the term $k_{A_0P}\exp(\Delta G_{A_0F_X}/RT)$) and thermal repopulation of P* (from F_X), followed by transition from P* to P (the term $k_{PP}\exp(\Delta G_{PF_X}/RT)$). In further calculations, we use the following values for the rate constants and free energy gaps shown in Fig. 5: $1/k_{PP} = 1$ ns; $1/k_{A_0P} = 30$ ns; $1/k_{A_1P} = 21\ \mu$s; $\Delta G_{PF_X} \approx -650$ mV; $\Delta G_{A_0F_X} \approx -350$ mV; $\Delta G_{A_1F_X} \approx -100$ mV.

The kinetics of the $A_1^- \rightarrow P^+$ transition are described by two components with ~10- and 100-μs lifetimes (see Fig. 2, *B* and *C*). As an initial approximation, we use here the average time for the $A_1^- \rightarrow P^+$ transition, obtained according to equation

$$1/\tau^{av}_{A_1P} = k^{av}_{A_1P} = \frac{k^1_{A_1P}\cdot p_1 + k^2_{A_1P}\cdot p_2}{p_1 + p_2},$$

where $\tau^1_{A_1P} = 1/k^1_{A_1P}$, $\tau^2_{A_1P} = 1/k^2_{A_1P}$ are time constants of the stretched multiexponential fit of the kinetics of $P700^+$ reduction by A_1^-, and p_1, p_2 are their amplitudes. The $\tau^{av}_{A_1P}$ is 21.9 μs for a PS I core lacking F_A and F_B (Fig. 2 *B*) and it is 20.7 μs for a PS I core from the *rubA* mutant lacking F_X, F_A, and F_B (Fig. 2 *C*). Thus, we use 21 μs for the $A_1^- \rightarrow P^+$ transition.

Setting these parameters in Eq. 6 gives the estimate for the rate constant of $P700^+$ dark reduction in the absence of F_A and F_B,

$$(k_P^{Phy})_{no\ F_AF_B} \approx 0.01 + 49 + 1026 \approx 1075. \quad (7)$$

Each term here corresponds to the different pathway of $P700^+$ dark reduction as specified by Eqs. 3 or 6. Eq. 7 shows that the main route of the P^+ dark reduction ($\geq$90%) is due to electron transfer from A_1^- to $P700^+$. The estimated rate constant $(k_P^{Phy})_{no\ F_AF_B}$ corresponds to a lifetime of ~1 ms, which is identical to the measured value in a PsaC-deficient PS I core (Fig. 2 *B*). The relative contribution of each route is quite sensitive to the values of energy differences between different states, and change of $\Delta G_{A_1F_X}$ from -100 to -80 mV changes estimated lifetime of the transition to ~0.43 ms. Thus, in the case of wild-type PS I complexes in the absence of F_A and F_B, Eq. 6 is simplified to the approximate equation for the rate constant of the $P700^+$ dark reduction,

$$(k_P^{Phy})_{no\ F_A/F_B} \approx k_{A_1P}\exp(\Delta G_{A_1F_X}/RT). \quad (8)$$

Flash-induced reactions of wild-type PS I in the absence of all iron–sulfur clusters

In the case where F_X, F_A, and F_X are removed, Eq. 6 should be replaced by the equation,

$$(k_P^{Phy})_{no\ F_X} \approx k_{PP}\exp(\Delta G_{PA_1}/RT), + k_{A_0P}\exp(\Delta G_{A_0A_1}/RT) + k_{A_1P}.$$

Setting here the rate constants and free energy gaps shown in Fig. 5 ($1/k_{PP} = 1$ ns; $1/k_{A_0P} = 30$ ns; $1/k_{A_1P} = 21\ \mu$s; $\Delta G_{PA_1} = -550$ mV; $\Delta G_{A_0A_1} \approx -250$ mV), gives the estimate for the rate constant of $P700^+$ dark reduction in the absence of F_X,

$$(k_P^{Phy})_{no\ F_X} \approx 0.68 + 2271 + 47619 \approx 5 \times 10^4\ s^{-1}.$$

Thus, in the case of wild-type PS I complexes with F_X absent, the rate constant of the $P700^+$ dark reduction is approximately equal to k_{A_1P}.

TABLE 1 Values of the time constants and free energy differences for wild-type PS I and *menA* PS I used in the calculations of Fig. 7

	Wild-type PS I with		*menA* PS I with	
	F_X, F_B, F_A	no FeS	F_X, F_B, F_A	no FeS
$1/k_{A_0A_1}$	50 ps	50 ps	50 ps	50 ps
$1/k_{A_1F_X}$	100 ns	–	15 μs	–
$1/k_{F_XF_A}$	800 ns	–	800 ns	–
$1/k_{F_AF_B}$	500 ns	–	500 ns	–
$1/k_{F_BF_A}$	250 ns	–	250 ns	–
$1/k_{A_0P}$	30 ns	30 ns	30 ns	30 ns
$1/k_{A_1P}$	21 μs	21 μs	100 μs	100 μs
$1/k_{F_XP}$	500 ms	–	500 ms	–
$\Delta G_{A_0A_1}$	−250 mV	−250 mV	−385 mV	−385 mV
$\Delta G_{A_1F_X}$	−100 mV	–	35 mV	–
$\Delta G_{F_XF_A}$	−105 mV	–	−105 mV	–

Flash-induced reactions of wild-type PS I in the absence of A_1

In the case where A_1 is removed, Eq. 6 should be replaced by the equation (see Table 1 for values of the rate constants and redox potentials used to estimate $P700^+$ dark reduction here),

$$(k_P^{Phy})_{\text{no } A_1} \approx k_{pp}\exp(\Delta G_{PA_0}/RT)+k_{A_0P} \approx 3.3\times 10^7 + 10^4 \approx 3.3\times 10^7.$$

Thus, the ratio of two different pathways of $P700^+$ dark reduction depends on the free energy difference between these two acceptors and the ratio of the rate constants of direct electron transfer from these acceptors to P700. Changes in the free energy gaps between different states can cause noticeable differences in the observed time of the $P700^+$ decay and change the contribution of different routes.

These two pathways are equal when

$$(k_{A_1P}/k_{A_0P}) \times \exp(-\Delta G_{A_0A_1}/RT)=1.$$

From this we can estimate (taking $1/k_{A_0P}$ = 30 ns; $1/k_{A_1P}$ = 21 μs) that these two pathways would provide equal input into $P700^+$ dark reduction where the free energy gap between A_0 and A_1 would be about −170 mV.

Flash-induced reactions of wild-type PS I in the presence of iron–sulfur clusters

In the case of wild-type PS I with DCPIP and ascorbate as donor of electrons to P700, both F_A and F_B are involved in flash-induced transitions (see Fig. 4). Because the energy gap between P* and F_A/F_B is largest (see Fig. 4 *A*), the terms $\exp(-\Delta G_{PF_A}/RT)$ and $\exp(-\Delta G_{PF_B}/RT)$ play a dominant role in the denominator of Eq. 5. Assuming for simplicity that $\Delta G_{PF_A} \sim \Delta G_{PF_B}$, and multiplying both numerator and denominator by $\exp(\Delta G_{PF_A}/RT)$, we have

$$(k_P^{Phy})_{F_AF_B} \approx \frac{k_{pp}\exp(\Delta G_{PF_A}/RT)+k_{A_0P}\exp(\Delta G_{A_0F_A}/RT)+k_{A_1P}\exp(\Delta G_{A_1F_A}/RT)}{2}. \quad (10)$$

The absence of nanosecond components in the kinetics of $P700^+$ dark reduction indicates that, in the absence of the bound iron–sulfur clusters, there is no significant contribution by A_0^-.

Expression for the ratio of two different pathways

It is important to note that the relative contribution of each route is quite sensitive to the values of energy differences between different states. Indeed, from Eqs. 2–4, we can write the ratio of two different pathways of the $P700^+$ dark reduction,

$$\frac{\text{Pathway via } A_1}{\text{Pathway via } A_0} \approx \frac{k_{A_1P}L_{PA_1}}{k_{A_0P}L_{PA_0}} \equiv \frac{k_{A_1P}\exp(-\Delta G_{A_0A_1}/RT)}{k_{A_0P}}. \quad (9)$$

As before, we can consider various routes of electron transfer that contribute to the effective rate constant of $P700^+$ decay. Setting rate constants and free energy gaps shown in Fig. 4 *A* ($1/k_{PP}$ = 1 ns; $1/k_{A_0P}$ = 30 ns; $1/k_{A_1P}$ = 21 μs; ΔG_{PF_A} = −755 mV; $\Delta G_{A_0F_A}$ = −455 mV; $\Delta G_{A_1F_A}$ = −205 mV) in Eq. 10, gives the estimate for the rate constant of $P700^+$ dark reduction,

$$(k_P^{Phy})_{F_AF_B} \approx (0 + 0.9 + 18.2)/2 \approx 9.6\ s^{-1}. \quad (11)$$

Each term here corresponds to the different pathway of $P700^+$ dark reduction as specified by Eq. 10. Eq. 11 shows that the main route of the P^+ dark reduction is due to electron transfer from F_A/F_B to A_1 and then to P700, whereas the routes involving A_0 and P* constitute less than 10%. The lifetime given by Eq. 11 is ~105 ms, which is close to the 107-ms value shown experimentally (Fig. 2 *A*).

Thus, in the case of wild-type PS I in the presence of DCPIP and ascorbate, Eq. 10 is simplified to the approx-

imate expression for the rate constant of $P700^+$ dark reduction,

$$(k_P^{Phy})_{F_AF_B} \approx \frac{k_{A_1P}\exp(\Delta G_{A_1F_A}/RT)}{2}. \quad (12)$$

Using Eq. 12, we can estimate the free energy gap between A_1 and F_A/F_B for $1/(k_P^{Phy})_{F_AF_B} = 108$ ms and $1/k_{A_1P} = 0.021$ ms,

$$\Delta G_{A_1F_A} \sim 60 \cdot \log\left(\frac{2(k_P^{Phy})_{F_AF_B}}{k_{A_1P}}\right) \sim -205 \text{ mV}.$$

Plastoquinone-9-containing PS I complexes

When phylloquinone is replaced by plastoquinone-9 in the A_1 binding site, we should expect, as a first approximation, that all rate and equilibrium constants not connected with A_1 are the same in wild-type and *menA* PS I complexes, and only the reactions of A_1 with other electron carriers are modified.

Flash-induced reactions of plastoquinone-9-containing PS I in the absence of iron–sulfur clusters

In the absence of iron–sulfur clusters (*menB/rubA* double mutant lacking F_X, F_A, and F_B), the kinetics of $P700^+$ dark reduction in PS I complexes is significantly slower than that in comparable wild-type PS I complexes.

As discussed earlier, the observed microsecond components with lifetimes of 26 and 362 μs in the F_X-deficient PS I cores (Fig. 3 *C*) are assigned to the back reaction between A_1^- and $P700^+$. As before, we use here the approximation of an average time for the $A_1^- \rightarrow P^+$ transition, obtained according to equation

$$\frac{1}{\tau_{A_1P}^{av}} = k_{A_1P}^{av} = \frac{k_{A_1P}^1 \cdot p_1 + k_{A_1P}^2 \cdot p_2}{p_1 + p_2}$$

The $\tau_{A_1P}^{av}$ is 94.5 μs for a PS I core lacking F_A and F_B (Fig. 3 *B*), and it is 98.9 μs for a PS I core from the *rubA* mutant lacking F_X, F_A, and F_B (Fig. 2 *C*). Thus, in future calculations, we use $\tau_{A_1P}^{av} = 100$ μs for the $A_1^- \rightarrow P^+$ transition in cases where plastoquinone-9 occupies the A_1 binding site. This value is close to the 200 μs lifetime measured by Iwaki and Itoh (1994) in the case when high-potential quinones are incorporated into the A_1 site.

These estimates indicate that in comparable preparations, the lifetime of the charge-separated state in an iron–sulfur-deficient PS I core is longer when plastoquinone-9 rather than phylloquinone is in the A_1 site. This finding is in apparent contradiction with the Moser–Dutton application (Moser et al., 1995) of Marcus theory (Marcus and Sutin, 1985), which connects electron transfer rate and distance between the electron carriers. Indeed, assuming that the reorganization energy and distance are the same for phylloquinone and ubiquinone, one can find that a small reorganization energy for the reaction between A_1 and P700 (0.3–0.7 eV) corresponds to the so-called inverted region in which the free energy difference is larger than the reorganization energy. In this case, K_{A_1P} should be larger in the PQ-containing complexes.

As a possible explanation for this apparent contradiction, one can propose that plastoquinone in the A_1 binding site assumes a position with a larger edge-to-edge distance from P700 than phylloquinone, making this rate of relaxation slower. Alternately, the presence of two methyl groups on plastoquinone-9, rather than a conjugated ring on phylloquinone, leads to a different environment with significantly larger reorganization energy.

Flash-induced reactions of menA *PS I in the absence of* F_A *and* F_B

As discussed above, the main 26- and 584-μs kinetic components of the kinetics of flash-induced absorbance changes in a *menA* PS I core stripped of PsaC (Fig 3 *B*), are assigned to the $P700^+$ A_1^- backreaction. The practical absence of much longer-lived components of the reaction $F_X^- \rightarrow P^+$ in mutant PS I in the absence of PsaC indicates that the main path of electron transfer to $P700^+$ is from A_1^- or A_0^-, not from F_X^- as in wild-type PS I.

Flash-induced reactions of menA *PS I in the presence of iron–sulfur clusters*

The kinetics of $P700^+$ dark reduction in the presence of the DCPIP and ascorbate in *menA* PS I complexes is faster than that in wild-type PS I complexes. To explain the observed fast kinetics of the $P700^+$, we can use the general model developed above.

From Eq. 4, we have the approximate equation for the observed rate constant of the $P700^+$ dark reduction in *menA* PS I in the presence of DCPIP and ascorbate (see also Eqs. 10– 12),

$$(k_P^{PQ})_{F_AF_B} \approx \frac{k_{A_1P}}{2L_{A_1F_A}}. \quad (13)$$

As in the case of Eq. 10, we assumed here that the energy gap between P* and F_A/F_B is largest and that $\Delta G_{PF_A} \approx \Delta G_{PF_B}$ Solving this equation for the $L_{A_1F_A}$ gives

$$L_{A_1F_A} \approx \frac{k_{A_1P}}{2(k_P^{PQ})_{F_AF_B}}. \quad (14)$$

The rate constant $(k_P^{PQ})_{F_AF_B}$ of $P700^+$ reduction observed in the presence of ascorbate and DCPIP (Fig. 3 *A*) corresponds to a lifetime of ~2.9 ms. The rate constant k_{A_1P} can be estimated from the *slow* components of the $P700^+$ reduction in *menA* PS I in the absence of the iron–sulfur clusters (Fig. 3 *C*). Using $1/k_{A_1P} = 100$ μs, we can estimate

from Eq. 14 the equilibrium constant of electron transfer between A_1 and F_A in mutant PS I,

$$L_{A_1F_A} \approx \frac{(10^6/100)}{2 \cdot (10^3/2.9)} \approx 14.5. \quad (15)$$

This corresponds to an ~ -70 meV energy gap between A_1 and F_A in plastoquinone-9-containing PS I complexes, indicating that functional E_m of A_1 is $\sim$ 35mV more oxidizing of that of F_x. This uphill direction of electron transfer from A_1 to F_X explains the absence of long-lived F_X components in the $P700^+$ dark reduction in mutant PS I complexes in the absence of PsaC (Fig 3 *B*). Figure 6 shows the energy profiles in RCs with different quinones, based on the above estimation of this free energy gap.

The presence of a thermodynamically-uphill electron transfer step in *menA* PS I could lead to a reinterpretation of the value of the rate constant of electron transfer from A_1 to F_x measured by Semenov et al. (2000). Indeed, the measured rate could depend on both the partitioning of electron between A_1 and F_X, and on the rate constant of electron transfer from F_x to F_A/F_B. Taking free energy gap between A_1 and F_X as +35 mV, we can estimate that, in this case, the rate constant of electron transfer from F_X to F_A could be $\sim$4 times larger than the measured value.

Mathematical modeling of electron transfer in PS I

The consistency of the above description of electron transport in mutant and wild-type PS I complexes with an intact set or a subset of iron–sulfur clusters F_X, F_B, and F_A and with the A_1 binding site occupied by phylloquinone or by plastoquinone can be checked further using mathematical modeling of respective processes with a system of differential equations. Figure 7 shows a series of theoretical curves calculated by solving a respective system of linear differential equations that describe the flash-induced transitions between different states in PS I (see Fig. 4),

$$d[A_1^-]/dt = -(k_{A_1P} + k_{A_1A_0} + k_{A_1F_X})[A_1^-] + k_{A_0A_1}[A_0^-] + k_{F_XA_1}[F_X^-], \quad \text{etc.},$$

where $[A_0^-]$, $[A_1^-]$, $[F_X^-]$ are the relative (per PS I complex) concentrations of the PS I states with reduced A_0, A_1, and F_X, respectively. This system of stiff differential equations was solved by using Matlab software. As initial conditions for this system, we assumed that A_0 is completely reduced after the short flash of light, i.e., $[A_0^-(0)] = 1$. The following values of rate constants and free energy differences (summarized in Table 1) were assumed to be the same in wild-type and mutant PS I during the calculation: $1/(k_{A_0A_1}) = 50$ ps; $1/k_{F_XF_A} = 0.8$ μs; $1/k_{F_AF_B} = 0.5$ μs; $1/k_{F_BF_A} = 0.25$ μs; $1/k_{A_0P} = 30$ ns; $1/k_{F_XP} = 500$ ms; $\Delta G_{F_XF_A} = -105$ meV. The following parameters were taken different in wild-type and mutant PS I during the calculation: $1/k_{A_1F_X} = 100$ ns in the wild-type and 15 μs in the *menA* mutant; $1/k_{A_1P} = 21$ μs in the wild type and 100 μs in the *menA* mutant; $\Delta G_{A_0A_1} = -250$ meV in the wild-type and -385 meV in the *menA* mutant; $\Delta G_{A_1F_X} = -100$ meV in the wild-type and +35 meV in the *menA* mutant. The rate constant for the backward transition be-

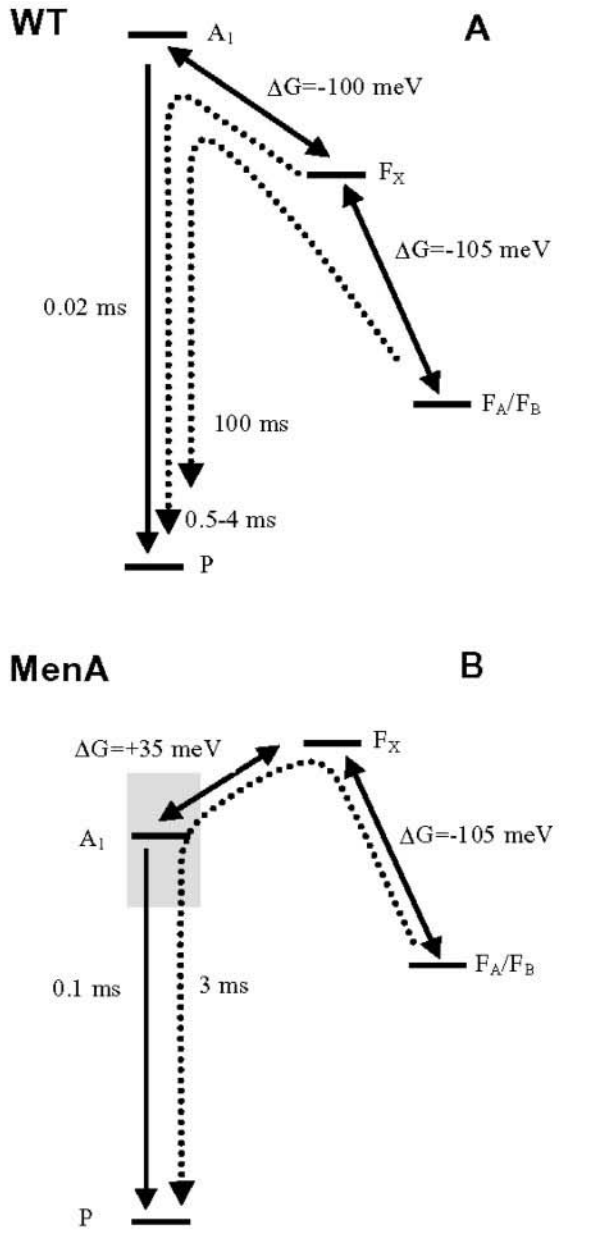

FIGURE 6 Schemes of electron transport in (*A*) phylloquinone and (*B*) plastoquinone containing PS I complexes. Shaded box in (*B*) indicates uncertainty in the value of estimated midpoint redox potential of A_1 due to the heterogeneity of the rate constant k_{A_1P}. The values depicted for the redox potentials and backreaction times are taken from the literature, and are either experimentally determined or deduced from thermodynamic or kinetic arguments (i.e., the E_m of A_0 and A_1).

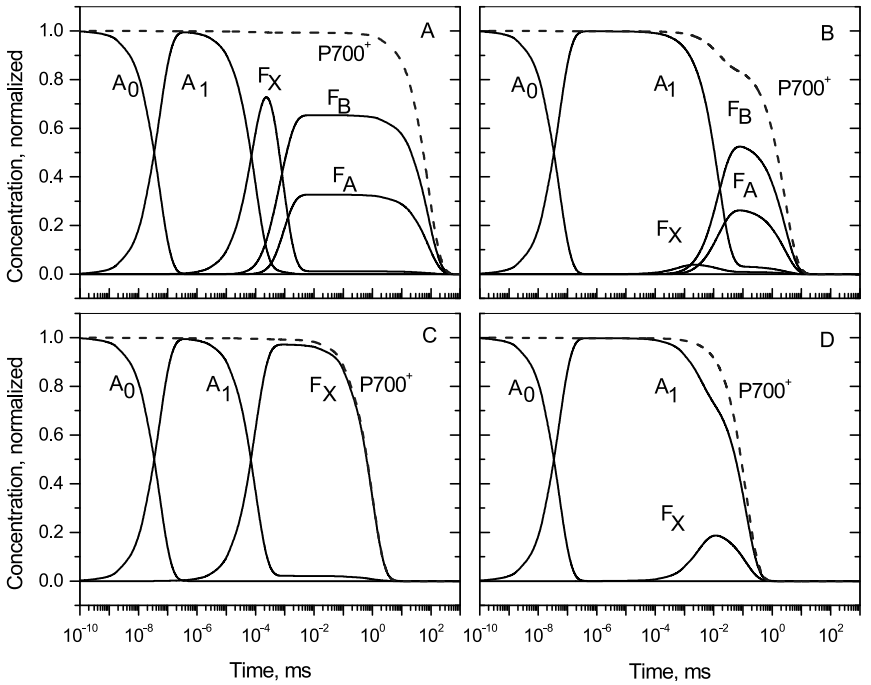

FIGURE 7 The theoretical time dependence of the relative concentrations of different electron carriers of the PS I complexes from (*A, C*) wild type and (*B, D*) *menA* mutant in the (*A, B*) presence of DCPIP and NaAsc and in the (*C, D*) absence of F_A and F_B. Rate and equilibrium constants used in calculation are shown in Table 1.

tween the given two states was calculated from the forward rate constant and respective equilibrium constant, estimated from the free energy difference for these two states (see Table 1). In simulating the effect of the removal of PsaC (Fig. 7 *C*, *D*), we assume $k_{F_XF_A} = 0$ to reflect that both F_A and F_B are absent.

Modeling of the kinetics of electron transfer in PS I complexes confirms that, in *menA* mutants, F_X is significantly less populated than in the case of the wild type, both in the presence of the iron–sulfur clusters (compare panels *A* and *B*) and in the absence of PsaC (compare panels *C* and *D*) in Fig. 7.

CONCLUSIONS

In wild-type PS I with phylloquinone in the A_1 site, the lifetime for $P700^+$ dark reduction is ~100 ms, whereas, in *menA* PS I with plastoquinone in the A_1 site, it is ~3 ms. The main component of $P700^+$ reduction in wild-type PS I in the absence of the F_A/F_B iron–sulfur clusters is due to a backreaction between F_X^- and $P700^+$ (via thermal repopulation of A_1), and is characterized by a lifetime of ~1 ms; the main component of $P700^+$ dark reduction in the absence of F_X (*rubA* mutant) is due to a backreaction between A_1^- and $P700^+$, and is characterized by two lifetimes of ~10 and 100 μs. In contrast, the main component of $P700^+$ reduction in *menA* PS I in the absence of the F_A/F_B iron–sulfur clusters is characterized by lifetimes of 26 and 584 μs; the main component of $P700^+$ dark reduction in the absence of F_X (*rubA/menB* double mutant) is characterized by similar lifetimes of ~26 and 362 μs. The slower backreaction from A_1^- to $P700^+$ in PS I complexes with plastoquinone in the A_1 site (average lifetime of ~100 μs) in comparison to wild-type PS I complexes with phylloquinone in the A_1 site (average lifetime of ~20 μs), may be explained by subtle differences in the position of plastoquinone in the A_1 site in comparison to phylloquinone or to differences in the reorganization energies caused by the presence of two methyl groups rather than a fully conjugated ring. The analysis of the kinetics of $P700^+$ decay in PS I complexes shows that the replacement of phylloquinone with plastoquinone-9 induces a significant decrease in the free energy gap between A_1 and F_A/F_B from ~−205 mV in wild-type PS I to ~−70 mV in mutant PS I. The +135 increase in the reduction potential of A_1 significantly accelerates the time of $P700^+$ dark reduction from ~100 ms in wild-type PS I to ~3 ms in *menA* PS I. The calculation of a +35 mV uphill electron transfer step between A_1 and F_X agrees with an assessment based on the Moser–Dutton application (Moser et al., 1995) of Marcus theory (Marcus and Sutin, 1985) that electron transfer between A_1 and F_X is thermodynamically unfa-

TABLE 2 Three-exponential deconvolution of the solution of differential equations for $P700^+$ shown in Fig. 7

	Time (ms)	Amplitude
Wild-type		
with F_X, F_B, F_A	**79.0**	**0.99**
F_X core	**0.95**	**1.0**
menA		
with F_X, F_B, F_A	**2.73**	**0.86**
F_X core	**0.13**	**1.0**

vorable by +12 to +95 mV when plastoquinone-9 substitutes for phylloquinone in PS I (Semenov et al., 2000).

This work was supported by a grant to J.H.G. from the National Science Foundation (MCB-0117079).

The authors thank Don Bryant, Gaozhong Shen, and Yumiko Sakuragi for constructing the *rubA/menB* double mutant.

REFERENCES

Brettel, K. 1997. Electron transfer and arrangement of the redox cofactors in Photosystem I. *Biochim. Biophys. Acta.* 1318:322–373.

Brettel, K., and J. H. Golbeck. 1995. Spectral and kinetic characterization of electron acceptor A_1 in a Photosystem I core devoid of iron–sulfur clusters F_X, F_B and F_A. *Photosyn. Res.* 45:183–193.

Brettel, K., and W. Leibl. 2001. Electron transfer in photosystem I. *Biochim. Biophys. Acta.* 1507:100–114

Fromme, P. 1999. Biology of Photosystem 1: structural aspects. *In* Concepts in Photobiology: Photosynthesis and Photomorphogenesis. G. S. Singhal, G. Renger, S. K. Sopory, and K.-D. Irrgang and Govindjee, editors, Narosa Publishing House/India, New Delhi, India. 181–220.

Golbeck, J. H. 1995. Resolution and reconstitution of Photosystem I. *In* CRC Handbook of Organic Photochemistry and Photobiology. P. S. Song, and W. Horspeels, editors. CRC Press, Bocca Raton, FL. 1423–1433.

Golbeck, J. H. 1999. A comparative analysis of the spin state distribution of *in vivo* and *in vitro* mutants of PsaC. A biochemical argument for the sequence of electron transfer in Photosystem I as $F_X \rightarrow F_A \rightarrow F_B \rightarrow$ ferredoxin/flavodoxin. *Photosyn. Res.* 61:107–149.

Guergova-Kuras, M., B. Boudreaux, A. Joliot, P. Joliot, and K. Redding 2001. Evidence for two active branches for electron transfer in photosystem I. *Proc. Natl. Acad. Sci. U.S.A.* 98:4437–4442.

Itoh S., M. Iwaki, and I. Ikegami. 1987. Extraction of vitamin K_1 from Photosystem I particles by treatment with diethyl ether and its effects on the A_1^- EPR signal and system I photochemistry. *Biochim. Biophys. Acta.* 893:508–516.

Iwaki, M., and S. Itoh. 1991a. Function of quinones and quinonoids in green-plant Photosystem I reaction center. *Adv. Chem. Ser.* 228:163–178.

Iwaki M., and S. Itoh. 1991b. Structure of the phylloquinone-binding (Q.vphi.) site in green plant photosystem I reaction centers: the affinity of quinones and quinonoid compounds for the Q.vphi. site. *Biochemistry.* 30:5347–5352.

Iwaki M., and S. Itoh. 1994. Reaction of reconstituted acceptor quinone and dynamic equilibration of electron transfer in the photosystem I reaction center. *Plant Cell Physiol.* 35:983– 993.

Iwaki M., S. Kumazaki, S. Yoshihara, T. Erabi, and S. Itoh. 1996. $\Delta G°$ dependence of the electron transfer rate in the photosynthetic reaction center of plant Photosystem I: Natural optimization of reaction between chlorophyll a (A_0) and quinone. *J. Phys. Chem. B.* 100: 10802–10809.

Johnson, T. W., G. Shen, B. Zybailov, D. Kolling, R. Reategui, S. Beauparlant, I. R. Vassiliev, D. A. Bryant, A. D. Jones, J. H. Golbeck, and P. Chitnis. 2000. Recruitment of a foreign quinone into the A1 site of photosystem I. I. Genetic and physiological characterization of phylloquinone biosynthetic pathway mutants in *Synechocystis* sp. PCC 6803. *J. Biol. Chem.* 275:8523–8530.

Johnson T. W., B. Zybailov, A. D. Jones, R. Bittl, S. Zech, D. Stehlik, J. H. Golbeck, and P. Chitnis. 2001. Recruitment of a foreign quinone into the A_1 site of Photosystem I. *In vivo* replacement of plastoquinone-9 by media-supplemented naphthoquinones in phylloquinone biosynthetic pathway mutants of *Synechocystis* sp. PCC 6803. *J. Biol. Chem.* 24: 39512–39521.

Jordan, P., P. Fromme, H. T. Witt, O. Klukas, W. Saenger, and N. Krau. 2001. Three dimensional structure of Photosystem I at 2.5 Å resolution. *Nature.* 411:909–917.

Ke, B. 2001. Photosynthesis. Kluwer Academic Press, Dordrecht, The Netherlands.

Klukas, O., W. D. Schubert, P. Jordan, N. Krauss, P. Fromme, H. T. Witt, and W. Saenger. 1999a. Localization of two phylloquinones, Q_K and Q'_K, in an improved electron density map of photosystem I at 4-Å resolution. *J. Biol. Chem.* 274:7361–7367.

Klukas, O., W. D. Schubert, P. Jordan, N. Krauss, P. Fromme, H. T. Witt, and W. Saenger. 1999b. Photosystem I, an improved model of the stromal subunits PsaC, PsaD, and PsaE. *J. Biol. Chem.* 274:7351–7360.

Kohlrausch, R. 1854. Theorie des elektrischen Rückstandes der Leidner Flasche. *Poggendorf's Ann. Physik Chem.* 91:56–82.

Kohlrausch, R. 1863. Über die elastiche Nachwirkung bei der Torsion. *Poggendorf's Ann. Physik Chem.* 119:337–368.

Manna, P., and P. R. Chitnis. 1999. Functional and molecular genetics in Photosystem I. *In* Concepts in Photobiology: Photosynthesis and Photomorphogenesis. G. S. Singhal, G. Renger, S. K. Sopory, K.-D. Irrgang and Govindjee, editors. Narosa Publishing House/India. New Delhi, India 221–263.

Marcus, R. A., and N. Sutin. 1985. Electron transfer in chemistry and biology, *Biochim. Biophys. Acta.* 811:265–322.

McMahon, B. H., J. D. Muller, C. A. Wraight, and G. U. Nienhaus. 1998. Electron transfer and protein dynamics in the photosynthetic reaction center. *Biophys. J.* 74:2567–2587.

Moser, C. C., C. C. Page, R. Farid, and P. L. Dutton. 1995. Biological electron transfer. *J. Bioenerg. Biomembr.* 27:263–274.

Schlodder, E., K. Falkenberg, M. Gergeleit, and K. Brettel. 1998. Temperature dependence of forward and reverse electron transfer from A_1^-, the reduced secondary electron acceptor in photosystem I. *Biochemistry.* 37:9466–9476.

Semenov, A. Y., I. R. Vassiliev, A. van Der Est, M. D. Mamedov, B. Zybailov, G. Shen, D. Stehlik, B. A. Diner, P. R. Chitnis, and J. H. Golbeck. 2000. Recruitment of a foreign quinone into the A1 site of photosystem I. Altered kinetics of electron transfer in phylloquinone biosynthetic pathway mutants studied by time-resolved optical, EPR, and electrometric techniques. *J. Biol. Chem.* 275:23429–23438.

Shen, G., M. L. Antonkine, A. J. van der Est, I. R. Vassiliev, K., Brettel, J. Zhao, D. Stehlik, D. Bryant, and J. H. Golbeck, 2002a. Assembly of [4Fe-4S] clusters in Photosystem I. II. Rubredoxin is required for assembly of F_X as shown by optical and EPR spectroscopy. *J. Biol. Chem.* 277:20355–20366.

Shen, G., J., Zhao, S., Reimer, Q., Cai, J. H. Golbeck, and D. A. Bryant, 2002b. Assembly of [4Fe-4S] clusters in Photosystem I. I. Inactivation of the gene encoding a membrane-associated rubredoxin in the cyanobacterium *Synechococcus* sp. PCC 7002, *J. Biol. Chem.* 277: 20343–20354.

Shinkarev, V. P. and C. A. Wraight. 1993. Electron and proton transfer in the acceptor quinone complex of reaction centers of phototrophic bacteria. *In The Photosynthetic Reaction Center* J. Deisenhofer and J. Norris. editors Vol. 1, Academic Press, New York. 193–255.

Vassiliev, I. R., Y. S. Jung, M. D. Mamedov, A. Y. Semenov, and J. H. Golbeck. 1997. Near-IR absorbance changes and electrogenic reactions in the microsecond-to-second time domain in photosystem I. *Biophys. J.* 72:301–315.

Vassiliev, I. R., M. Antonkine, and J. H. Golbeck. 2001a. Iron–sulfur clusters in type I reaction centers. *Biochim. Biophys. Acta.* 1507:139–160.

Vassiliev, I. R., B. Kjaerr, G. Schorner, H. V. Scheller, and J. H. Golbeck. 2001b. Photoinduced transient absorbance spectra of P840/$P840^+$ and the FMO protein in reaction centers of *Chlorobium vibrioforme. Biophys. J.* 81:382–393.

Yu, J., L. B., Smart, Y.-S., Jung, J. H. Golbeck, and L. McIntosh. 1995. Absence of PsaC subunit allows assembly of photosystem I core but prevents binding of PsaD and PsaE in *Synechocystis* sp. PCC 6803. *Plant Mol. Biol.* 29:311–342.

Zybailov, B., A. van der Est, S. G. Zech, C. Teutloff, T. W. Johnson, G. Shen, R. Bittl, D. Stehlik, P. R. Chitnis, and J. H. Golbeck. 2000. Recruitment of a foreign quinone into the A_1 site of Photosystem I. II. Structural and functional characterization of phylloquinone biosynthetic pathway mutants by electron paramagnetic resonance and electron-nuclear double resonance spectroscopy. *J. Biol. Chem.* 275: 8531–8539.